Nanodiamond Stability

DOI: 10.1002/ange.200501495

Thermodynamic Stability and Ultrasmall-Size Effect of Nanodiamonds**

Chengxin Wang, Jian Chen, Guowei Yang, and Ningsheng Xu**

Nano- and ultra-nanodiamonds have emerged as promising materials for various applications,[1–4] although their stabilization is still unclear.[5] Compared with graphite, diamond is a

[*] Dr. C. X. Wang, Prof. J. Chen, Prof. G. W. Yang, Prof. N. S. Xu
State Key Laboratory of Optoelectronic Materials and Technologies
School of Physics Science & Engineering
Zhongshan University
Guangzhou 510275 (P. R. China)
Fax: (+86) 8411-3692
E-mail: stsygw@zsu.edu.cn
stsxns@zsu.edu.cn

[**] We gratefully acknowledge support by the National Science Foundation of China (NSFC) under Grants No.50072022 & 10474140 and the National Natural Science Foundation of China (the Distinguished Creative Group Project).

Supporting information for this article is available on the WWW under http://www.angewandte.org or from the author.

metastable phase under atmospheric pressure according to the thermodynamic equilibrium phase diagram of carbon. However, it has been verified by experiments,[5–15] calculations,[16–19] and theory[20,21] that nanodiamonds with diameters of less than 5 nm are more stable than their graphitic counterparts. By calculating the structural energies (formation energies) of graphite, diamond, and fullerene on the basis of density functional theory, Barnard et al.[22] reported that the relative stability is dependent on the size of carbon clusters. For instance, diamond could be the stable phase of carbon clusters when the size is in the range of 1.9–5.2 nm. Thus, from the above studies, we conclude that a better understanding is required for two fundamental issues: 1) what relationship exists between size distribution and stability of nanodiamonds, and 2) what is the physical origin of the stability of nanodiamonds.

We have now studied the graphitization of nanodiamonds experimentally and theoretically. Interestingly, we found size-dependent graphitization of nanodiamonds, that is, the stability of nanodiamonds depends on size, and this implies that a nanosize effect is operative, remarkably similar to that of nanocavities.[23] Meanwhile, we established a thermodynamic model for the size effect on the basis of nanothermodynamic analysis.[20,24]

Commercial diamond nanoparticles with sizes of 5–6 nm and over 90% phase purity were annealed under a flow of Ar (purity $>99.99\%$) at atmospheric pressure and given temperatures. Annealing temperatures were in the range from room temperature (RT) to 1423 K, and annealing was performed for 2 h at each temperature. Transmission electron microscopy (TEM), selected-area electron diffraction (SAD), X-ray diffraction (XRD), Raman spectroscopy, and differential scanning calorimetry (DSC) were used to identify the graphitization of diamonds (for detailed analysis, see Supporting Information). The linewidth of the Raman spectrum as a function of nanodiamond size was calculated from the phonon-confinement model (Figure 1).[25] The inset to Figure 1 shows that the size of the residual nanodiamonds decreases from 5.5 to approximately 2.5 nm when the annealing temperature is elevated from RT to 1423 K. Figure 2a shows the bright-field TEM pattern of nanodiamonds annealed at 1423 K for 2 h. The size of the residual nanodiamonds is about 2.5 nm, and diamond nuclei are surrounded by an amorphous ring (see magnified view, top left in Figure 2a). These results indicate that graphitization starts at the surface region, on the basis of experiments by Enoki,[11] which are in good agreement with the above analysis. These experimental results reveal that the graphitization of nanodiamonds is size-dependent, and nanodiamonds smaller than 3 nm are more stable than graphite in graphitization at moderate temperature, that is, the phase stability of nanodiamonds is verified experimentally from the viewpoint of diamond-to-graphite transformation. This new size effect differs distinctly from the widely accepted nanosize and quantum-size effects that occur when the size confining a condensed-matter system is so small that it becomes comparable to the lattice distance.[26] A similar nanosize effect was reported for the shrinkage of nanocavities upon ion-beam irradiation.[23] A general symmetry relationship between nanoparticles and nanocavities can thus be established, as illustrated schematically in Figure 2b.

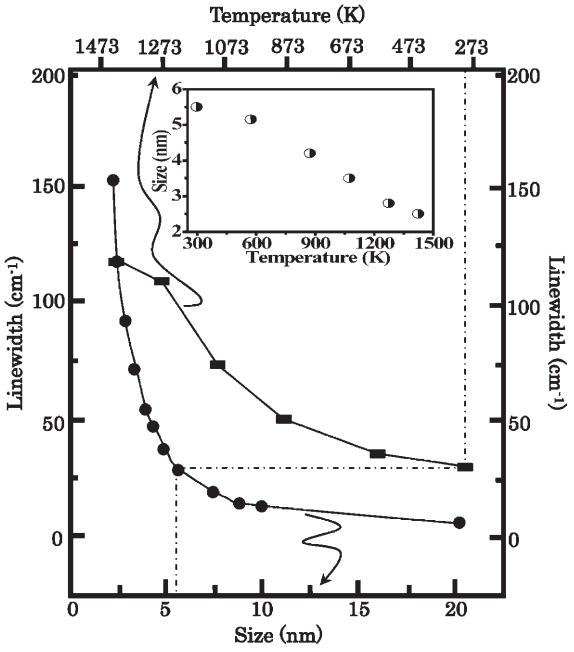

Figure 1. F_{2g} mode linewidth of Raman spectra versus annealing temperature (experimental values, ■) and variation of linewidth with particle sizes of 2.3, 2.5, 3.0, 3.5, 4.0, 4.5, 5.0, 5.7, 7.5, 8.8, 10.0, and 20.0 nm, based on the phonon-confinement model (calculated values, ●). The dash-dot line indicates the determination of particle size. The inset shows a plot of particle size versus annealing temperature.

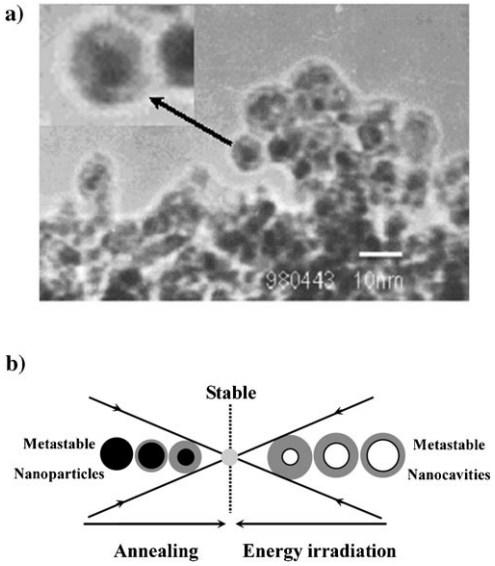

Figure 2. a) TEM images of 5–6 nm nanodiamonds after annealing at 1423 K for 2 h show that the size of the residual nanodiamonds is about 2.5 nm. b) The symmetry relationship between nanoparticles (left) and nanocavities (right) reveals that a similar nanosize effect operates in condensed-matter systems at the nanometer scale.

To provide a better understanding of the size effect in terms of thermodynamics, based on the equilibrium phase diagram of carbon[26] and thermodynamic analysis at the

nanometer scale,[20,24] we performed a thermodynamic study, taking into account the capillary effect of the nanometer-sized curvature of diamond and graphite nanoparticles by the Laplace–Young equation. Under these assumptions of spherical and quasi-isotropic nanocrystals, the nanosize-curvature-induced interior pressure of the nanodiamonds, ΔP, is expressed by the Laplace–Young equation as $\Delta P = 4\gamma/d$, where γ and d are the surface tension and the diameter of spherical nanodiamonds, respectively. In view of the thermodynamic phase diagram of carbon,[27] the phase-equilibrium-line function $P(T)$ of the diamond–graphite phase transition in the bulk is approximately expressed by Equation (1).[20]

$$P^{be}(T)\ (\text{in Pa}) = 2.01 \times 10^6\, T + 2.02 \times 10^9 \quad (1)$$

$P^{be}(T)$ denotes the phase-equilibrium-line pressure (external pressure) in the bulk. On the basis of the liquid-drop model, the phase equilibrium line on the nanometer scale must be scaled taking into account the radius of curvature. This dependence is universal for all elements in the periodic table. Naturally, the phase equilibrium line on the nanometer scale is a function of temperature, pressure, and nanocrystal radius. The phase-equilibrium-line equation is expressed by Equation (2).[20]

$$P^{ne}(T,d)\ (\text{in Pa}) = 2.01 \times 10^6 T + 2.02 \times 10^9 - \frac{4\gamma}{d} \quad (2)$$

$P^{ne}(T,d)$ is the phase-equilibrium-line pressure (external pressure) under consideration of the radius of curvature of the nanodiamonds. In our case (under atmospheric pressure), if nanodiamonds are the stable phase, the functional relationship must fulfil the condition $4\gamma/d + 10^5 \geq 2.01 \times 10^6 T + 2.02 \times 10^9$. Thus, when $4\gamma/d + 10^5 = 2.01 \times 10^6 T + 2.02 \times 10^9$, we attain a new phase-equilibrium line for the size–temperature relationship, as shown in Figure 3a. These theoretical predictions of the nanodiamond stability are in good agreement with our experimental results. Furthermore, we calculated the Gibbs free energy of the graphitization of nanodiamonds by considering the nanosize-induced interior pressure. The Gibbs free energy is expressed as a function of radius r_g, pressure P, and temperature T [Eq. (3)].[20]

$$\Delta G(r_g,P,T)\ (\text{in J}) = \left(\frac{4}{3}\pi {r_g}^3\, \Delta g/V_{mg} + 4\pi {r_g}^2 \gamma_g\right) f(\theta) \quad (3)$$

V_{mg}, γ_g, and θ are the molar volume of graphite ($5.187 \times 10^{-6}\ m^3$), the surface energy of graphite ($0.55\ J\,m^{-2}$),[21a] and a contact angle,[20] respectively. Here, $f(\theta)$ is the so-called heterogeneous factor (in the range from 0 to 1) and can be expressed by $(1-\cos\theta)^2(2+\cos\theta)/4$, and Δg is the molar-volume Gibbs free energy, which is relative to dimension according to Equation (4), when the phase transition takes place near the phase-equilibrium line.

$$\Delta g\ (\text{in J}) = \Delta V\left(2.01 \times 10^6 T + 2.02 \times 10^9 - \frac{4\gamma}{d} - 1 \times 10^5\right) \quad (4)$$

ΔV ($1.77\ m^3\,mol^{-1}$)[20] is the molar volume difference between diamond and graphite. When $\frac{\partial \Delta G(r)}{\partial r} = 0$, the critical size of graphitization nuclei is obtained [Eq. (5)].

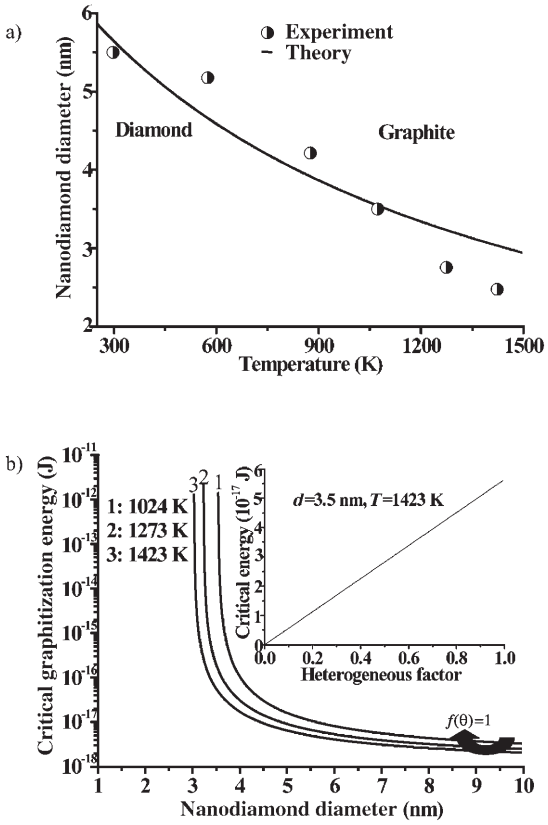

Figure 3. a) Phase-equilibrium line of diamond–graphite size–temperature relationship, which suggests that the stability of residual nanodiamonds is a function of size at a certain temperature. b) Relative curves of the diameters of nanodiamonds and the Gibbs free energy of the nanodiamond graphitization for various annealing temperatures and a given heterogeneous factor, which reveals that a definite threshold size exists for the graphitization of nanodiamonds at a given annealing temperature. The inset shows the relationship between the heterogeneous factor and the critical energy of graphitization.

$$r_g^*\ (\text{in m}) = \frac{2\gamma}{\left(\frac{4\gamma}{d} + 1 \times 10^5 - 2.01 \times 10^6 T - 2.02 \times 10^9\right)\frac{V_{mg}}{\Delta V}} \quad (5)$$

Accordingly, we attain the relationship curve between size of the residual crystalline nanodiamond nuclei and the Gibbs free energy of graphitization for various annealing temperatures and heterogeneous factors (Figure 3b). Clearly, the Gibbs free energy of graphitization increases with decreasing nanodiamond size at a given temperature. For various annealing temperatures, there are corresponding thresholds of the size of residual nanodiamonds in graphitization, and this suggests that only the surface region of the nanodiamond particles is graphitized at a given temperature, and then graphitization proceeds inward on further elevation of annealing temperature at the expense of nanodiamond phase, as proved by the appearance of bands for graphitic structures in the Raman spectrum and X-ray diffraction (see Supporting Information). Thus, graphitization would display a staircase behavior with increasing annealing temperature,

due to the surface-curvature effect of the diamond and graphite nanoparticles. For example, the threshold diameters of the residual nanodiamonds are about 3.5 and 3 nm at annealing temperatures of 1073 and 1423 K. Therefore, graphitization hardly proceeds further when the size of the residual nanodiamonds reaches 3.5 and 3 nm at annealing temperatures of 1073 and 1423 K, respectively, which are consistent with our experiments. For comparison, the relationship curve between the graphitization energy and heterogeneous factor is shown as inset in Figure 3b. Similarly, we calculated the relationship curve between the annealing temperature and the probability of diamond-to-graphite transition. According to the general expression of the phase transformation probability,[28] the probability of graphitization is expressed as $f_g = \exp[-(E_a/RT)] - \exp[-(E_a - \Delta g)/RT]$, where R and E_a are the gas constant and the activation energy (212 kJ mol^{-1}),[29] respectively, and Δg is relative to dimension and defined by Equation (4). The resulting relationship curves between annealing temperature and graphitization probability are shown in Figure 4. Apparently, threshold

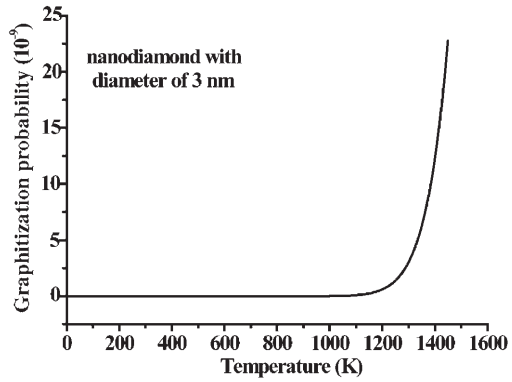

Figure 4. Dependence of the nanodiamond graphitization on annealing temperature for nanodiamonds of a given size. The transition from diamond to graphite almost stops for nanodiamonds with diameters of 3 nm at an annealing temperature of 1300 K.

temperatures exist for the graphitization of nanodiamonds of various sizes. For instance, graphitization of residual nanodiamonds with a size of 3 nm stops when the threshold temperature is about 1300 K. These theoretical results therefore indicate that the surface tension induced by the nanosized curvature of nanodiamonds is the physical origin of their stability and the size effect in nanodiamond graphitization. Accordingly, a thermodynamic approach on the nanoscale also seems applicable to the shrinkage of nanocavities.

In summary, nanodiamonds smaller than 3 nm were experimentally verified to be more stable than graphite from the viewpoint of nanodiamond graphitization. The relationship between the size of residual nanodiamonds and the critical energy of graphitization at given temperatures was studied theoretically on the basis of the size–temperature phase diagram, by taking into account the capillary effect of nanodiamonds, and revealed the dependence of graphitization on nanodiamond diameter and annealing temperature. Both experiment and theory suggested that the nanometer-sized curvature of nanodiamonds is the physical origin of the stability of nanodiamonds.

Received: April 30, 2005
Revised: August 26, 2005
Published online: October 24, 2005

Keywords: carbon · graphitization · nanostructures · phase diagrams · thermodynamics

[1] N. R. Greiner, D. S. Phillips, J. D. Johnson, F. Volk, *Nature* **1988**, *333*, 440–442.
[2] W. B. Choi, J. Liu, M. T. McClure, A. F. Myers, V. V. Zhirnov, J. J. Cuomo, J. J. Hren, *J. Vac. Sci. Technol. B* **1996**, *14*, 2050–2055.
[3] W. B. Choi, J. J. Cuomo, V. V. Zhirnov, A. F. Myers, J. J. Hren, *Appl. Phys. Lett.* **1996**, *68*, 720–722.
[4] E. I. Givargizov, V. V. Zhirnov, A. N. Stepanova, E. V. Rakova, A. N. Kiselev, P. S. Plekhanov, *Appl. Surf. Sci.* **1995**, *87*/88, 24–30.
[5] N. S. Xu, J. Chen, S. Z. Deng, *Diamond Relat. Mater.* **2002**, *11*, 249–256.
[6] P. W. Chen, Y. S. Ding, Q. Chen, F. L. Huang, S. R. Yun, *Diamond Relat. Mater.* **2000**, *9*, 1722–1725.
[7] S. Jiao, A. Sumant, M. A. Kirk, D. M. Gruen, A. R. Krauss, O. Auciello, *J. Appl. Phys.* **2001**, *90*, 118–122.
[8] S. T. Lee, H. Y. Peng, X. T. Zhou, N. Wang, C. S. Lee, I. Bello, Y. Lifshitz, *Science* **2002**, *297*, 104–106.
[9] Y. Gogotsi, S. Welz, D. A. Ersoy, M. J. McNallan, *Nature* **2001**, *411*, 283–287.
[10] Yu. V. Butenko, V. L. Kuznetsov, A. L. Chuvilin, V. N. Kolomiichuk, S. V. Stankus, R. A. Khairulin, B. Segall, *J. Appl. Phys.* **2000**, *88*, 4380–4388.
[11] T. Enoki, *Phys. Solid State* **2004**, *46*, 651–656.
[12] B. L. V. Prasad, H. Sato, T. Enoki, *Phys. Rev. B* **2000**, *62*, 11209–11218.
[13] A. E. Aleksenskiĭ, M. V. Baĭdakova, A. Ya. Vul', V. Yu. Davydov, Yu. A. Pevtsova, *Phys. Solid State* **1997**, *39*, 1007–1015.
[14] J. W. Ager III, D. K. Veirs, G. M. Rosenblatt, *Phys. Rev. B* **1991**, *43*, 6491–6499.
[15] S. Prawer, J. L. Peng, J. O. Orwa, J. C. McCallum, D. N. Jamieson, L. A. Bursill, *Phys. Rev. B* **2000**, *62*, 16360–16363.
[16] P. Badziag, W. S. Verwoerd, W. P. Ellis, N. R. Greiner, *Nature* **1990**, *343*, 244–245.
[17] N. W. Winter, F. H. Ree, *J. Comput.-Aided Mater. Des.* **1998**, *5*, 279–294.
[18] J. Y. Raty, G. Galli, *Nat. Mater.* **2003**, *2*, 792–795.
[19] H. R. Francis, N. W. Winter, J. N. Glosli, J. A. Viecelli, *Physica B* **1999**, *265*, 223–229.
[20] C. X. Wang, Y. H. Yang, N. S. Xu, G. W. Yang, *J. Am. Chem. Soc.* **2004**, *126*, 11303–11306; C. X. Wang, Y. H. Yang, G. W. Yang, *J. Appl. Phys.* **2005**, *97*, 066104–066106; Y. C. Zhang, C. X. Wang, G. W. Yang, *J. Phys. Chem. B* **2004**, *108*, 2589–2593.
[21] a) D. S. Zhao, M. Zhao, Q. Jiang, *Diamond Relat. Mater.* **2002**, *11*, 234–236; b) Q. Jiang, J. C. Li, G. Wilde, *J. Phys. Condens. Matter* **2000**, *12*, 5623–5627.
[22] A. S. Barnard, S. P. Russo, I. K. Snook, *J. Chem. Phys.* **2003**, *118*, 5094–5097.
[23] X. F. Zhu, *J. Phys. Condens. Matter* **2003**, *15*, L253–L261.
[24] C. X. Wang, Y. H. Yang, Q. X. Liu, G. W. Yang, *J. Phys. Chem. B* **2004**, *108*, 728–731; C. X. Wang, Q. X. Liu, G. W. Yang, *Chem. Vap. Deposition* **2004**, *10*, 280–283; C. X. Wang, Y. H. Yang, G. W. Yang, *Appl. Phys. Lett.* **2004**, *84*, 3034–3036.
[25] H. Richter, Z. P. Wang, L. Ley, *Solid State Commun.* **1981**, *39*, 625–629; J. Chen, S. Z. Deng, J. Chen, Z. X. Yu, N. S. Xu, *Appl. Phys. Lett.* **1999**, *74*, 3651–3653.

[26] G. Bertsch, *Science* **1997**, *277*, 1619 – 1619.
[27] F. P. Bundy, W. A. Bassett, M. S. Weathers, R. J. Hemley, H. U. Mao, A. F. Goncharov, *Carbon* **1996**, *34*, 141 – 153.
[28] J. B. Wang, G. W. Yang, *J. Phys. Condens. Matter* **1999**, *11*, 7089 – 7094.
[29] V. L. Solozhenko, V. Z. Turkevich, O. O. Kurakevych, *J. Phys. Chem. B* **2002**, *106*, 6634 – 6637.

